Scaling behavior and strain dependence of in-plane elastic properties of graphene

J. H. Los, A. Fasolino, and M. I. Katsnelson[1]

[1] *Radboud University, Institute for Molecules and Materials, Heyendaalseweg 135, 6525AJ Nijmegen, The Netherlands*

(Dated: August 24, 2015)

We show by atomistic simulations that, in the thermodynamic limit, the in-plane elastic moduli of graphene at finite temperature vanish with system size L as a power law $L^{-\eta_u}$ with $\eta_u \simeq 0.325$, in agreement with the membrane theory. Our simulations clearly reveal the size and strain dependence of graphene's elastic moduli, allowing comparison to experimental data. Although the recently measured difference of a factor 2 between the asymptotic value of the Young modulus for tensilely strained systems and the value from *ab initio* calculations remains unsolved, our results do explain the experimentally observed increase of more than a factor 2 for a tensile strain of only a few permille. We also discuss the scaling of the Poisson ratio, for which our simulations disagree with the predictions of the self-consistent screening approximation.

Mechanical and structural properties of graphene form an intriguing and highly non-trivial aspect of its physics. The structure of a two-dimensional (2D) material embedded in a 3D space gives room to special features, related to large out-of-plane deformations, in particular thermal ripples [1–9] and static ripples and wrinkles [10]. A crucial difference with 3D (or strictly 2D) crystals is that, for graphene, out-of-plane atomic displacements h and in-plane displacements $\mathbf{u}$ have different wavevector dependence of the energy cost in the long wavelength limit $q \to 0$, namely $\propto q^2$ and $\propto q$ respectively, the latter being the normal behavior for acoustic phonons. Hence, at finite temperature, the long wavelength out-of-plane fluctuations are much larger than the in-plane ones, so that at some small wavevector q the first anharmonic coupling term of the form uh^2 will dominate over the "normal" harmonic terms u^2, with important consequences for the elastic behavior[8, 9, 11–14]. In particular, the wavevector dependence of the anharmonic coupling strength leads to expect a power law behavior of the size dependence of the elastic properties.

Contrary to the temperature dependence [15, 16], so far the size dependence of the in-plane elastic moduli of graphene has been hardly studied nor measured [17] until recent experiments seem to indicate that such a size dependence does exist for graphene [18, 19]. From indentation experiments on graphene drums with sizes of the order of 1 μm, the Young modulus Y was found to vary between 250 N/m and 700 N/m with increasing strain [19], the latter value being much higher than the currently accepted value for flat sheets of $\sim$ 340 N/m obtained in previous measurements [17] or *ab initio* calculations [20].

Here we study the size dependence of the in-plane elastic moduli of graphene at room temperature T=300 K by means of atomistic Monte Carlo (MC) simulations based on the realistic interatomic potential LCBOPII [21], as used in previous works [2, 4, 15]. We obtain explicit expressions for the size and strain dependence of graphene's in-plane elastic moduli, providing a benchmark and tools for the analysis of experiments for systems of any size.

Theoretically, the mentioned size dependence has been studied within the continuum elastic theory of thin plates and membranes, described by the Hamiltonian [22]:

$$H = \frac{1}{2}\int d\mathbf{r}\big(\kappa(\nabla^2 h)^2 + \lambda u_{\alpha\alpha}^2 + 2\mu u_{\alpha\beta}^2\big) \qquad (1)$$

where $\mathbf{r}$ is the 2D position vector, κ is the bending rigidity, λ and μ are Lamé coefficients, with μ the shear modulus, and

$$u_{\alpha\beta} = \frac{1}{2}(\partial_\alpha u_\beta + \partial_\beta u_\alpha + \partial_\alpha h\, \partial_\beta h) \qquad (2)$$

is the strain tensor.

The harmonic approximation neglects the non-linear h^2 term, decoupling the bending and stretching modes. Then the correlation functions for out-of-plane displacements, $H_0(q) = \langle |h_\mathbf{q}|^2\rangle_0$, and for in-plane displacements, $D_{u,0}^{\alpha\beta}(q) = \langle u_{\alpha\mathbf{q}}^* u_{\beta\mathbf{q}}\rangle_0$, can be derived by Gaussian integration [8, 9]:

$$H_0(q) = \frac{k_B T}{\kappa q^4} \qquad (3)$$

and:

$$D_{u,0}^{\alpha\beta}(q) = \frac{P_{\alpha\beta}(\mathbf{q})k_B T}{(\lambda+2\mu)q^2} + \frac{(\delta_{\alpha\beta} - P_{\alpha\beta}(\mathbf{q}))k_B T}{\mu q^2} \qquad (4)$$

with $P_{\alpha\beta}(\mathbf{q}) = q_\alpha q_\beta/q^2$. The average height fluctuation behaves as $\langle h^2\rangle_0 = \sum_\mathbf{q}\langle |h_\mathbf{q}|^2\rangle_0 \sim L^2$, implying instability of a membrane as a flat phase.

Due to the large out-of-plane fluctuations, however, the harmonic behavior is not valid for small q and one has to keep the h^2 term in eq. 2. Since H remains quadratic in u, these degrees of freedom can still be integrated out. This leads to a Hamiltonian in Fourier space which is a function of $h_\mathbf{q}$ only [9]:

$$\tilde{H} = \frac{1}{2}\sum_\mathbf{q} \kappa q^4 |h_\mathbf{q}|^2 + \frac{Y}{8}\sum_{\mathbf{q},\mathbf{k},\mathbf{k}'} R(\mathbf{q},\mathbf{k},\mathbf{k}') h_\mathbf{k} h_{\mathbf{q}-\mathbf{k}} h_{\mathbf{k}'} h_{-\mathbf{q}-\mathbf{k}'} \qquad (5)$$

where Y is the 2D Young modulus and $R(\mathbf{q},\mathbf{k},\mathbf{k}') = (\mathbf{q}\times\mathbf{k})(\mathbf{q}\times\mathbf{k}')/q^4$. The anharmonic, quartic term reduces the height fluctuations, stabilizing the flat phase, effectively described by a renormalized bending rigidity $\kappa_R(q) \sim q^{-\eta}$ with positive η. Hence, the height correlation $H(q)$ for $q \to 0$ has the same form as $H_0(q)$ in eq. 3, but with κ replaced by $\kappa_R(q)$ [11]. Likewise, $D_u^{\alpha\beta}(q)$ can be described by renormalized $\lambda_R(q), \mu_R(q) \sim q^{\eta_u}$ in eq. 4 with $\eta_u > 0$. From rotational invariance it follows that η and η_u should satisfy the scaling relation $\eta_u = 2 - 2\eta$ [23].

Within the self-consistent screening approximation (SCSA) [13], the exponent was estimated as $\eta \simeq 0.821$ [13]; next-order corrections reduce it slightly to $\eta \simeq 0.789$ [14]. A renormalization group approach gives $\eta = 0.849$ [24] and MC simulations for self-avoiding membranes $\eta \simeq 0.72$ [25]. With $\eta > 0$, $\langle h^2\rangle \sim L^{2-\eta}$, is much smaller than $\langle h^2\rangle_0 \sim L^2$ for large L, stabilizing the flat phase.

Although it is *a priori* not obvious whether the membrane theory applies to an atomic-layer-thick 2D crystal like graphene, atomistic MC simulations confirm the scaling behavior of $H(q)$ with $\eta \simeq 0.85$[4]. The scaling of in-plane elastic moduli, however, has not yet been studied nor confirmed for graphene. Contrary to κ_R which increases with increasing system size, making the membrane more resistant against bending, λ_R and μ_R decrease with system size. Hence, if graphene follows the membrane theory, the in-plane elastic moduli vanish for large system sizes, an unthinkable situation for 3D crystals!

For a 2D system, the 2D bulk modulus B, the uniaxial modulus C_{11} and Y are related to λ and μ as:

$$B = \lambda + \mu\ , \quad C_{11} = B + \mu \quad \text{and} \quad Y = \frac{4B\mu}{B+\mu} \qquad (6)$$

implying that B, C_{11} and Y scale as λ and μ. Another relevant quantity is the 2D Poisson ratio ν:

$$\nu = \frac{B-\mu}{B+\mu} \qquad (7)$$

The SCSA predicts a universal, negative Poisson ratio $\nu = -1/3$ for $L \to \infty$ [13], as later confirmed by MC simulation of self-avoiding membranes [26]. For graphene, however, so far only positive values were reported ($\nu = 0.15 - 0.46$) [15, 27, 28].

In Fig.1 we show the in-plane correlation function $D_u^{\alpha\alpha}(q)$ ($\alpha = x, y$) calculated by NPT MC simulations at pressure $P = 0$ and $T = 300$ K with isotropic volume fluctuations for roughly square samples of $N = 37888$ atoms using periodic boundary conditions. Besides displacement moves we apply also collective wave moves for small q as in Ref. 4. For the calculation of $D_u^{\alpha\alpha}(q) = \langle|u_q^\alpha|^2\rangle = (1/N)\langle|\sum_i^N u_{i\alpha}\exp(i\mathbf{q}\mathbf{r}_{i,0})|^2\rangle$ with $\{r_{i,0}\}$ the ground state positions, the in-plane displacement field was scaled as $u_{i\alpha} = s r_{i\alpha} - r_{i\alpha,0}$ where $s = \sqrt{A_0/A}$ scales the area A at T=300 K to the ground state area A_0 of a flat sample. The behavior of $D_u^{xx}(q)$ for small q is consistent with a power law with exponent $\eta_u \simeq 0.3$, indicating that graphene follows the membrane theory also for in-plane correlations.

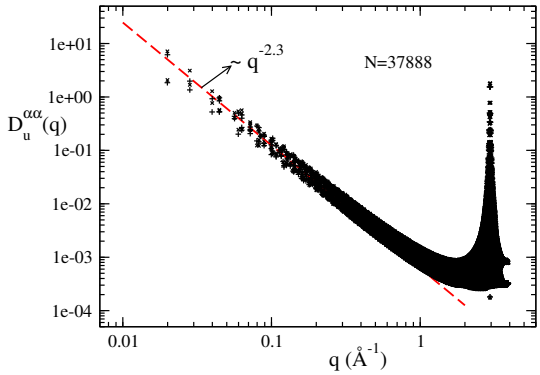

FIG. 1. Correlation functions $D_u^{\alpha\alpha}$ ($\alpha = x, y$) for in-plane displacements u_{ix} (x) and u_{iy} (+). The scaling exponent is consistent with $D_u^{\alpha\alpha} \sim q^{-2-\eta_u}$ with $\eta_u = 2 - 2\eta = 0.3$, using $\eta \simeq 0.85$ [24] (dashed line).

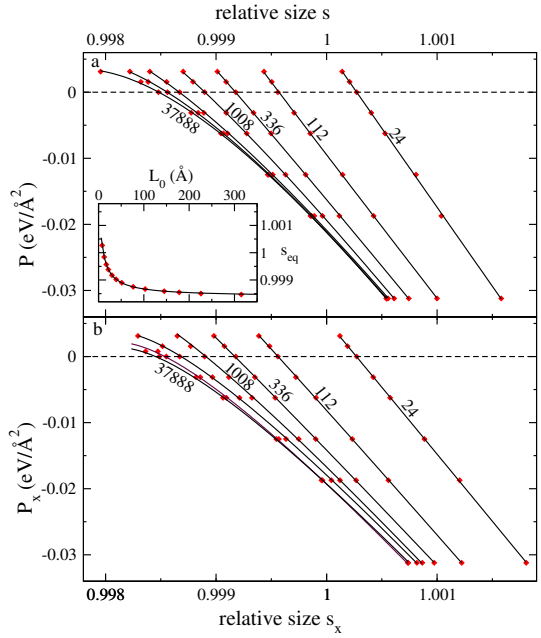

FIG. 2. Pressure as a function of size in NPT simulations (symbols) with (a) isotropic and (b) uniaxial size fluctuations for approximately square systems with N =24, 112, 336, 1008, 4032, 12096 and 37888 atoms. The lines are best fits to eq. 11. The inset gives the equilibrium sizes $s_{eq} = s(P = 0)$ (symbols) as a function of L_0 and the fit (solid line) according to the expression in Table I.

The size and strain dependence of the elastic properties can be computed simultaneously by NPT MC simulations for different sizes with isotropic area fluctuations at several pressures P. The resulting average area A gives the

equation of state (EOS), $A(P)$ and thus also $P(A)$ from which B can be calculated as:

$$B = -A\frac{\partial P}{\partial A} = -\frac{s}{2}\frac{\partial P}{\partial s} \tag{8}$$

where $s = L/L_0$ is the relative linear system size with $L_0 = \sqrt{N/\rho_0}$ the ground state system size, $\rho_0 \simeq 0.3819$ Å^{-2} being the 2D ground state atomic density of graphene. To obtain both B and C_{11}, we also performed NPT simulations for uniaxial pressure P_x, applying fluctuations of L_x in the x-direction, while keeping L_y fixed. Then C_{11} follows from:

$$C_{11} = -L_x\left.\frac{\partial P_x}{\partial L_x}\right|_P = -s_x\left.\frac{\partial P_x}{\partial s_x}\right|_P \simeq -s_x\left.\frac{\partial P_x}{\partial s_x}\right|_{s_y=s_{eq}} \tag{9}$$

where $s_\alpha = L_\alpha/L_{\alpha,0}$, with $L_{\alpha,0}$ ($\alpha = x, y$) the ground state dimensions, and where $s_{eq} = s(P = 0)$ is the equilibrium size obtained from the isotropic NPT simulations at $P = 0$. The subscript "P" in eq. 9 indicates that L_y should be taken equal to $s_y = s(P)$ resulting from isotropic NPT simulations at pressure P and that P_x should be varied around P. However, since we verified that the dependence of $\partial P_x/\partial s_x$ on s_y is very weak we adopted the last approximation in eq. 9, which is exact for $P = 0$.

The results are shown in Fig. 2. The inset shows that the previously found negative thermal expansion [15] is also size dependent, but tending to a constant for large L_0. On the basis of Fig. 2a, with the slope $\partial P/\partial s = 2B/s$ tending to a constant for large s, we propose the phenomenological relation for $B(s)$

$$B(s) = \frac{s\,(B_{eq}/s_{eq} + CD(s - s_{eq}))}{1 + D(s - s_{eq})} \tag{10}$$

where B_{eq} is the equilibrium value at $P = 0$. Substitution of eq. 10 into eq. 8 and integration yields the EOS:

$$P(s) = -\frac{2}{D}\left(\frac{B_{eq}}{s_{eq}} - C\right) ln\,(1 + D(s - s_{eq})) - 2C(s - s_{eq}) \tag{11}$$

Similarly, we write

$$C_{11}(s_x) = \frac{s_x\left(C_{11,eq}/s_{eq} + \tilde{C}\tilde{D}(s_x - s_{eq})\right)}{1 + \tilde{D}(s_x - s_{eq})} \tag{12}$$

which substituted in eq. 9 gives an equation for $P_x(s_x)$ similar to eq. 11 but with s, B_{eq}, C and D replaced by s_{eq}, $C_{11,eq}/2$, $\tilde{C}/2$ and $\tilde{D}$. This form allows the excellent fits shown in Fig. 2, providing B_{eq} and $C_{11,eq}$ as a function of L_0. In the left panels of Fig. 3 (left panels) we show that both B and C_{11} vanish for large L_0, decreasing as a power law $\sim L^{-\eta_u}$, with $\eta_u \simeq 0.325$ (insets). The right panels give the corresponding results for Y and ν at $P = 0$, calculated using eqs. 6 and 7. Note that, according to LCBOPII, the in-plane elastic moduli of graphene

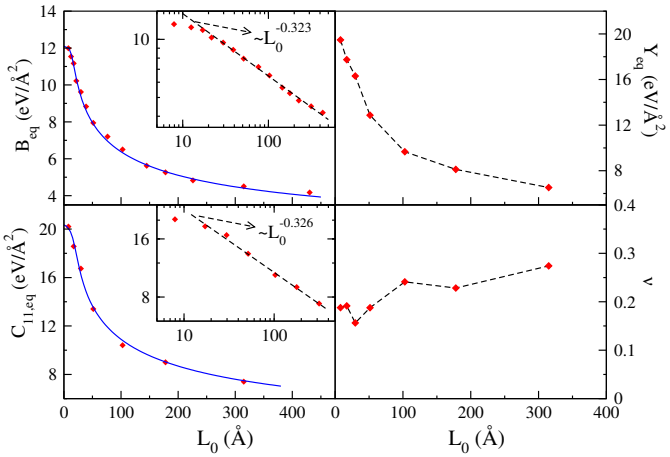

FIG. 3. Equilibrium bulk modulus B_{eq}, uniaxial modulus $C_{11,eq}$, Young modulus Y_{eq} and Poisson ratio ν as a function of system size L_0. The insets in log-log scale demonstrate the power law behavior. The solid lines are fits according to the expressions in Table I. Dashed lines in the right panels are guides to the eye.

at $T = 0$ K are $B = 12.69$ eV/Å^2 and $\mu = 9.26$ eV/Å^2, yielding $Y = 21.41$ eV/Å^2 = 343 N/m and $\nu = 0.156$, in agreement with *ab initio* data [20] and with the small size limit in Fig. 3 where $Y \simeq 314$ N/m. By simulations at 1 K for $N = 24$ we verified that the remaining difference is due to temperature.

Interestingly, the power law decrease of B, C_{11} and Y_{eq} as a function of L_0 sets in from $L_0 \simeq 20$ Å, a value twice smaller than the Ginzburg critical value $L^* = 2\pi\sqrt{16\pi\kappa^2/(3Yk_BT)} \simeq 40$ Å (using $\kappa \simeq 1.1eV$ [2]) expected from membrane theory [11]. The Poisson ratio ν for small sizes is close to its bare value and increases up to 0.275 for larger L_0, against the SCSA prediction $\nu = -1/3$. Since the scaling of B and μ is consistent with the SCSA, it is very unlikely that ν will reach the value -1/3 for $L_0 \to \infty$, as the outcome of eq. 7 only depends on the prefactors.

We can also calculate Y as a function of tensile strain, using eqs. 10 and 12 with the best fit parameters. We should use the $B(s)$ and $C_{11}(s_x)$ at equal pressure by solving $P_x(s_x) = P(s)$ for s_x at given s. Due to the approximation in eq. 9, $s_x \neq s$ unless $s = s_{eq}$. An approximation of $s_x(s)$ is given in Table I. The $Y(s)$ obtained from the data of Fig. 2 are shown in Fig. 4 for different sizes. Symbols mark the results at $s = s_{eq}$. Notice the strong increase of $Y(s)$ for large sizes. For $N = 37888$ ($L_0 \simeq 315$ Å), Y increases from ~ 100 N/m at $s_{eq} \simeq 0.9985$ to 220 N/m at $s = 0.9995$, i.e. more than a factor 2 for a strain $\epsilon = s - s_{eq} = 0.001$ (0.1 %)! This strong dependence is in full qualitative agreement with the recent experimental claims [18, 19]. A quantitative comparison will be discussed below.

Since B_{eq} and $C_{11,eq}$, as well as s_{eq}, C, D, $\tilde{C}$ and $\tilde{D}$ turn out to depend smoothly on L_0, we can approximate

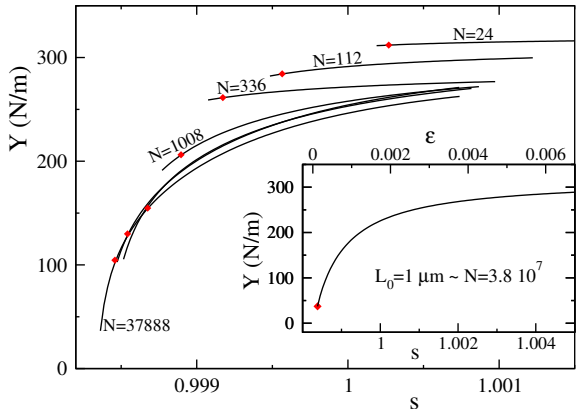

FIG. 4. Young modulus $Y(s)$ as a function of s for sample sizes as in Fig. 2 with symbols for $s = s_{eq}$. The inset shows $Y(s)$ for a size of 1 μm ($N \simeq 3.8 \times 10^7$), calculated using eqs. 10 and 12 and the expressions in Table I. The upper axis of the inset gives the strain $\epsilon = s - s_{eq}$.

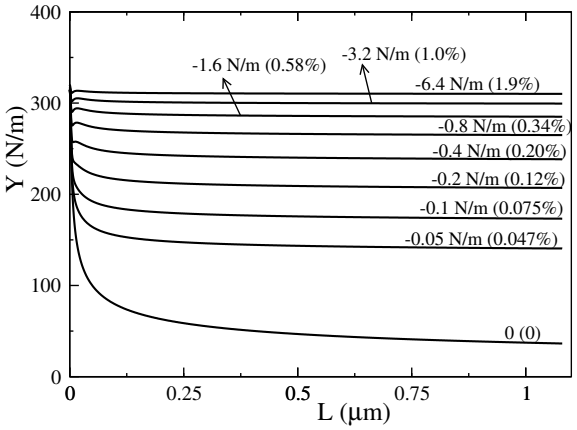

FIG. 5. Young modulus Y as a function of L_0 for the indicated values of the pressure P. The value in brackets is the corresponding strain $\epsilon = s - s_{eq}$.

$s_{eq} = 0.99838 + \frac{4.295\ 10^{-3}}{1+0.1814 L_0^{0.94}}, \quad D = \frac{592.3+1.2510^{-2} L_0^2}{1+1.2510^{-5} L_0^2},$
$B_{eq} = \frac{12.1-5.69\ 10^{-3} L_0^2+28.6(L_0/14.14)^4 L_0^{-0.325}}{1.0+(L_0/14.14)^4}, \quad C = 12.1,$
$C_{11,eq} = \frac{20.35-7.597\ 10^{-3} L_0^2+1.47\ 10^{-4} L_0^3+48.1(L_0/31.62)^4 L_0^{-0.325}}{1.0+(L_0/31.62)^4},$
$\tilde{C} = 20.35, \quad \tilde{D} = \frac{309.2+0.1597 L_0^2}{1+1.4510^{-4} L_0^2}, \quad s_x(s) = 1.15(s - s_{eq}) + s_{eq}$

TABLE I. Size dependent parameters for $B(s)$ and $C_{11}(s_x)$ according to eqs. 10 and 12 for L_0 in Å. B_{eq}, $C_{11,eq}$, C and $\tilde{C}$ are in eV/Å^2, other quantities are dimensionless.

all parameters by the functions of L_0 given in Table I. These expressions apply to any size and give appropriate asymptotics with C ($\tilde{C}$) equal to $\partial P/\partial s$ ($\partial P_x/\partial s_x$) for the smallest system (N=24).

The inset of Fig. 4 shows the resulting $Y(s)$ for a size $L_0 = 1$ μm ($\sim N = 3.8 \times 10^7$ atoms). At zero strain (symbol) Y is only 30 N/m, becoming almost a factor 10 larger at 0.5 % tensile strain, where it approaches its asymptotic value. Although the suppression of anharmonicity found here goes very fast as a function of strain, it clearly deviates from membrane theory within the SCSA, where a complete suppression of anharmonicity occurs for tensile strain of 0.01 % [29], two orders of magnitude lower than our atomistic simulations.

Finally, the size dependence of Y with tensile strain at negative pressures is displayed in Fig. 5. Tensile stress of 0.05 N/m, corresponding to ∼0.05 % strain, suppresses the anharmonic effects, and thus the power law decay, for $L_0 > 0.25$ μm. As a consequence, Y is a factor ~ 4 larger than Y_{eq} for a system of 1 μm. Subsequently, increasing the stress by a factor 10 yields a strain of ∼0.25 % and $Y \simeq 275$ N/m. This variation of Y with strain corresponds to recent experimental data.[19] The factor 2 difference in both lower and upper bound of Y, however, with an experimental upper value Y =700 N/m, remains unexplained and requires further investigations. We note that our values of the bare elastic moduli agree with the experimental phonon spectrum [30, 31] of graphite, where anharmonic effects are suppressed by interlayer interactions.

In conclusion, we have shown by atomistic simulations that the in-plane elastic moduli of graphene vanish with size as $L_0^{-\eta_u}$ with $\eta_u \simeq 0.325$, confirming that graphene follows membrane theory within the SCSA in this respect. The critical exponent η_u, together with the independent estimate of $\eta \simeq 0.85$ [4], supports the scaling relation $\eta_u = 2 - 2\eta$. In contrast, our results do not support the SCSA prediction $\nu = -1/3$ for $L \to \infty$. We remark that $\nu = -1/3$ in eqs. 6 and 7 leads to $B_R = -\lambda_R$ and $\lambda_R = 2B_R - C_{11}$, implying that λ_R should be negative for stability while in Fig. 3 $2B_R - C_{11,R}$ remains positive for any L_0. We also find that suppression of anharmonicity requires a tensile strain 10-50 times larger than predicted by SCSA.

This research has received funding from the European Union Seventh Framework Programme under grant agreement n604391 Graphene Flagship.

[1] J. C. Meyer, A. K. Geim, M. I. Katsnelson, K. S. Novoselov, T. J. Booth, and S. Roth, Nature **446**, 60 (2007).
[2] A. Fasolino, J. H. Los, and M. I. Katsnelson, Nat. Mater. **6**, 858 (2007).
[3] N. Abedpour, M. Neek-Amal, R. Asgari, F. Shahbazi, N. Nafari, and M. R. R. Tabar, Phys. Rev. B **76**, 195407 (2007).
[4] J. H. Los, M. I. Katsnelson, O. V. Yazyev, K. V. Zakharchenko, and A. Fasolino, Phys. Rev. B **80**, 121405(R) (2009).
[5] R. C. Thompson-Flagg, M. J. Moura, and M. Marder, Europhys. Lett. **85**(4), 46002 (2009).

[6] R. Zan, C. Muryn, U. Bangert, P. Mattocks, P. Wincott, D. Vaughan, X. Li, L. Colombo, R. S. Ruoff, B. Hamilton, and K. S. Novoselov, Nanoscale **4** (10), 3065 (2012).

[7] W. Gao and R. Huang, Journal of the Mechanics and Physics of Solids **66**, 42 (2014).

[8] M. I. Katsnelson and A. Fasolino, Acc. Chem. Res. **46**, 97 (2013).

[9] M. I. Katsnelson, *Graphene: Carbon in Two Dimensions* (Cambridge Univ. Press, Cambrigde, 2012), Chap. 9.

[10] W. Zhu, T. Low, V. Perebeinos, A. A. Bol, Y. Zhu, H. Yan, J. Tersoff, and P. Avourisa, NanoLett. **12**, 3431 (12012).

[11] D. R. Nelson, T. Piran, and S. Weinberg, (eds) *Statistical Mechanics of Membranes and Surfaces*, World Scientific, Singapore, 2004.

[12] D. R. Nelson and L. Peliti, J. Physique **48**, 1085 (1987).

[13] P. Le Doussal and L. Radzihovsky, Phys. Rev. Lett. **69**, 1209 (1992).

[14] D. Gazit, Phys Rev E **80**(4), 041117 (2009).

[15] K. V. Zakharchenko, M. I. Katsnelson, and A. Fasolino, Phys. Rev. Lett. **102**(4), 046808 (2009).

[16] S. Chen and D.C. Chrzan, Phys. Rev. B **84**(19), 195409 (2011).

[17] C. Lee, X. Wei, J. W. Kysar, and J. Hone, Science. **321**, 385 (2008).

[18] G. López-Polín, C. Gómez-Navarro, V. Parente, F. Guinea, M. I. Katsnelson, F. Pérez-Murano, and Julio Gómez-Herrero, Nature Physics 11, 26-31 (2015).

[19] G. López-Polín, M. Jaafar, R. Roldán, C. Gómez-Navarro, and J. Gómez-Herrero, arXiv:1504.05521 (2015).

[20] D. Sanchez-Portal, E. Artacho, J. M. Soler, A. Rubio, and P. Ordejon, Phys. Rev. B **59**, 12678 (1999).

[21] J. H. Los, L. M. Ghiringhelli, E. J. Meijer, and A. Fasolino, Phys. Rev. B **72**, 214102 (2005).

[22] L. D. Landau and E. M. Lifshitz, *Theory of Elasticity*, (Oxford: Pergamon, 1970).

[23] J. A. Aronovitz and T. C. Lubensky, Phys. Rev. Lett. **60**, 2634 (1988).

[24] J.-P. Kownacki and D. Mouhanna, Phys. Rev. E **79**, 040101(R) (2009).

[25] M. J. Bowick, S. M. Catterall, M. Falcioni, G. Thorleifsson, and K. N. Anagnostopoulos, J. Phys. I (Paris) **6**, 1321 (1996).

[26] M. Bowick, A. Cacciuto, G. Thorleifsson, and A. Travesset, Phys. Rev. Lett. **87**, 148103 (2001).

[27] E. Cadelano, P. L. Palla, S. Giordano, and L. Colombo, Phys. Rev. Lett. **102**, 235502 (2009).

[28] G. Cao, Polymers **6**, 2404 (2014).

[29] R. Roldán, A. Fasolino, K. V. Zakharchenko, and M. I. Katsnelson, Phys. Rev. B **83**, 174104 (2011).

[30] R. Nicklow, N. Wakabayashi, and H. G. Smith, Phys. Rev. B **5**, 4951 (1972).

[31] L. J. Karssemeijer and A. Fasolino, Surf. Sci. **605**, 1611 (2011).